Generation of transmitochondrial cybrids in cancer cells

Ruth Soler-Agesta[1,2], Cristina Ripollés-Yuba[1], Joaquín Marco-Brualla[1], Raquel Moreno-Loshuertos[1], Ai Sato[2], Manuel Beltrán-Visiedo[2], Lorenzo Galluzzi[2,3,4,*] and Alberto Anel[1,*]

[1]University of Zaragoza/Aragón Health Research Institute, Biochemistry and Molecular and Cell Biology, Zaragoza, Spain; [2]Department of Radiation Oncology, Weill Cornell Medical College, New York, NY, United States; [3]Sandra and Edward Meyer Cancer Center, New York, NY, USA; [4]Caryl and Israel Englander Institute for Precision Medicine, New York, NY, USA.

*Co-senior authors, correspondence to Lorenzo Galluzzi (deadoc80@gmail.com) or Alberto Anel (anel@unizar.es)

Keywords: 22Rv1 cells; cancer metabolism; immunity; DU-145 cells; mtDNA; rho^0 cells.

Abstract

At odds with historical views suggesting that mitochondrial functions are largely dispensable for cancer cells, it is now clear that mitochondria have a major impact on malignant transformation, tumor progression and response to treatment. Mitochondria are indeed critical for neoplastic cells not only as an abundant source of ATP and other metabolic intermediates, but also as gatekeepers of apoptotic cell death and inflammation. Interestingly, while mitochondrial components are mostly encoded by nuclear genes, mitochondria contain a small, circular genome that codes for a few mitochondrial proteins, ribosomal RNAs and transfer RNAs. Here, we describe a straightforward method to generate transmitochondrial cybrids. i.e., cancer cells depleted of their mitochondrial DNA and reconstituted with intact mitochondria from another cellular source. Once established, transmitochondrial cybrids can be stably propagated and are valuable to dissect the specific impact of the mitochondrial genome on cancer cell functions.

1. Introduction

More than a century ago, the German physiologist Otto Warburg was the first to report that malignant lesions exhibit a higher propensity to take up glucose as compared to normal tissues, a process that is commonly known as the "Warburg effect" {Warburg, 1923 #284;Warburg, 1924 #283;Thompson, 2023, 37990075;Koppenol, 2011, 21508971}. Such a seminal discovery not only laid the foundation for an improved understanding of how cancer cells reconfigure their metabolism in support of tumor progression and resistant to therapy, *de facto* spearheading a vivid line of investigation attempting to target tumor metabolism for therapeutic purposes {Stine, 2022, 34862480;Galluzzi, 2013, 24113830}, but also provided the rationale for the development of a diagnostic tool that is commonly employed for clinical cancer management, [^{18}F]-fluorodeoxyglucose positron emission tomography ([^{18}F]-FDG PET) scans {Schwenck, 2023, 37258875;Yankeelov, 2014, 25113842}. That said, Warburg postulated that malignant cells largely rely on glucose for bioenergetic metabolism as a consequence of mitochondrial dysfunction {Warburg, 1956, 13351639;Warburg, 1956, 13298683}, a possibility that has now been invalidated {Vaupel, 2021, 33347611;Vyas, 2016, 27471965;Zong, 2016, 26942671}. Indeed, accrued glucose uptake by malignant cells appears to mainly fuel anabolic (rather catabolic) metabolism in support of lipid and nucleotide biosynthesis (which are crucial for accelerated proliferation), mitochondrial ATP remaining the major source of energy {Locasale, 2011, 21804546;DeBerardinis, 2020, 32694689;Lunt, 2011, 21985671;Vander Heiden, 2009, 19460998}. Moreover, mitochondrial metabolism at large – including catabolic and anabolic components thereof – is fundamental for all steps of oncogenesis, including malignant transformation, tumor progression and response to treatment {Porporato, 2018, 29219147;Hanahan, 2022, 35022204;Hanahan, 2011, 21376230;Petroni, 2021,

33338426}Finally, mitochondrial integrity is paramount for the inhibition of cell-intrinsic (as mediated by regulated cell death) {Yuan, 2023, 38110635;Diepstraten, 2022, 34663943;Vitale, 2023, 37100955} as well as cell-extrinsic (as mediated by the host immune system) oncosuppression {Marchi, 2023, 35879417;Vringer, 2023, 36447047;Kroemer, 2023, 37880100;Catalán, 2015, 25949869;Yamazaki, 2020, 32747819}.

Of note, while the majority of mitochondrial constituents including all lipids and the vast majority of proteins is synthesized based on nuclear genetic information, mitochondria contain a small, circular genome that replicated independent of genomic DNA and encode a few mitochondrial proteins, ribosomal RNAs and transfer RNAs {Medini, 2020, 32857636;Neupert, 2016, 27058308;Rackham, 2022, 35459860}. Moreover, (1) mtDNA inheritance in daughter cells is largely stochastic {Gustafsson, 2016, 27023847}; and (2) most importantly, cell contains several mitochondrial DNA (mtDNA) molecules, which are not necessarily identical to each other (a scenario commonly referred to as heteroplasmy) {Stewart, 2021, 32989265}. Coupled to the fact that mtDNA replication is more prone to errors than genomic DNA (gDNA) replication {Roy, 2022, 35341749}, these observations imply that individual mtDNA molecules have a high propensity to accumulate mutations, which can stochastically accumulate in daughter cells with a potentially pathogenic decreased in heteroplasmy {Kopinski, 2021, 34045735}.

Importantly, while the CRISPR/Cas9 technology has rendered experimental gDNA alterations routinary not only in cultured cells but also in animals {Villiger, 2024, 38308006}, artificially altering mtDNA in cells and organisms remain challenging. To some degree, such obstacle can be partially circumvented by the generation of “transmitochondrial cybrids”, i.e., cells depleted of their own mtDNA (generally referred to as rho^0 (or ρ^0) cells) that reconstituted with intact mitochondria from another cellular source (**Figure 1**). Here, we detail a straightforward protocol

to generate prostate cancer “transmitochondrial cybrids” based on human prostate cancer DU-145 cells as recipient cells and human prostate 22Rv1 cells as donor cells. With minimal variations, we expect this method to be simply adaptable to other recipient and donor cancer cell lines of human and murine origin.

2. Materials

2.1. Common disposables (*see Note 1*)

- Cell culture flasks 25 cm^2 (#90026, Techno Plastic Products)
- Cell culture flasks 75 cm^2 (#90076, Techno Plastic Products)
- Corning® 96-well Clear Flat Bottom Polystyrene TC-treated Microplates, 5 per Bag, with Lid, Sterile (#3598, Corning)
- Costar® 24-well Clear TC-treated Multiple Well Plates, Individually Wrapped, Sterile (#09-761-146, Corning)
- Falcon® 15 mL High Clarity PP Centrifuge Tube, Conical Bottom, with Dome Seal Screw Cap, Sterile (#352096, Corning)
- Falcon® 50 mL High Clarity PP Centrifuge Tube, Conical Bottom, with Dome Seal Screw Cap, Sterile (#352070, Corning)
- Flex-Tube® 1.5 mL (#022364111, Eppendorf)

2.2. Cells and reagents (*see Note 1*)

- 10x TBE Buffer (Tris/Boric Acid/EDTA), 1 L (#1610733, BioRad)
- Buffer A: 10 mM Tris, 1 mM EDTA, 0.32 M sucrose, pH 7.4
- Complete DMEM: Gibco™ Dulbecco's Modified Eagle's Medium (DMEM), high glucose (4.5 g/L), GlutaMAX™ Supplement, supplemented with 10 % FBS, 10,000 U/mL penicillin and 10 mg/mL streptomycin
- Complete RMPI 1640 medium: Gibco™ RPMI 1640 Medium, supplemented with 10 % FBS, 10,000 U/mL penicillin and 10 mg/mL streptomycin.

- Ethanol 99 % (#100983, Supelco)
- Ethidium Bromide (#E8751, Sigma-Aldrich) (***see Note 2***)
- Fetal Bovine Serum (FBS, #F7524, Sigma-Aldrich)
- Gibco™ Dulbecco's Modified Eagle's Medium (DMEM), high glucose (4.5 g/L), GlutaMAX™ Supplement (#10566016, Thermo-Fisher Scientific)
- Gibco™ RPMI 1640 Medium (#11875093, Thermo-Fisher Scientific)
- Human 22Rv1 prostate cancer cells (#CRL-2505, ATCC)
- Human DU-145 prostate cancer cells (#HTB-81, ATCC)
- LightCycler® FastStart DNA Master^{PLUS} SYBR Green I (#03515869001, Roche)
- MOPS (#M1254, Sigma-Aldrich)
- Nuclease free water (#MC1191, Promega)
- Penicillin-Streptomycin, 10,000 U/mL Penicillin, 10 mg/mL Streptomycin (#P06-07100, PAN-Biotech)
- Polyethylene glycol (PEG) solution (#P7181, Sigma-Aldrich)
- QIAamp® DSP DNA Blood Mini Kit (#61104, Qiagen)
- qPCR primers (**Table 1**)
- *SacI*-HF® restriction enzyme kit (#R3156S, New England BioLabs®)
- Sodium pyruvate (#P5280, Sigma-Aldrich)
- Sucrose (#S9378, Sigma-Aldrich)
- TopVision Agarose (#R0491, ThermoFisher Scientific)
- Trypan Blue Solution, 0.4 % (#T10282, Invitrogen)
- Trypsin 0.25 %/ 1 mM EDTA 4Na in HBSS, w/o: Ca and Mg, w: Phenol red (#P10-029100, PAN-Biotech)

- Uridine (#U3750, Sigma-Aldrich)

2.3. Equipment (*see Note 1*)

- 5331 Mastercycler Gradient Thermal Cycler (Eppendorf)
- Azure 600® Imager (Azure Biosystems)
- CK inverted microscope (Olympus)
- Fisherbrand™ Horizontal Electrophoresis Systems (#FB-SB-710, Fisher Scientific)
- Homogenizer, motor-driven rotor (Bosch)
- LightCycler® 2.0 System (Roche)
- MCO-18AIC(UV) CO_2 Incubator for Cell Culture (Sanyo)
- MicrofugeR 22R Centrifuge (Beckman Coulter™)
- NanoVue™ Plus Spectrophotometer (GE Healthcare)
- Telstar™ PV-30/70 Vertical Laminar Air Flow Cabinet (Telstar™)
- Tissue Grinders-homogenizer, Glass Vessel, 2 mL (#196102, Deltalab)
- Tissue Grinders-homogenizer, Plunger-serrated Tip, 2 mL (#196302, Deltalab)

2.4. Software (*see Note 1*)

- Excel (Microsoft)
- LightCycler® v. 4.1 (Roche)
- Primer Express 2.0 (Applied Biosystems)
- Prism v. 10.0.1 (GraphPad)

- ## 3. Methods

3.1. ρ^0 cell generation (*see Notes 3 and 4*)

1. Wild-type (WT) DU-145 cells are maintained in culture using complete DMEM supplemented with 50 µg/mL uridine and 100 µg/mL pyruvate (***see Notes 5 and 6***).
2. Treat 2-3 X 10^6 DU-145 cells with 500 ng/mL ethidium bromide for a total of 10 days, refreshing ethidium bromide-containing medium every 48 hours (***see Notes 7 and 8***).

3.2. Quantification of mtDNA by qPCR

The degree of mtDNA depletion in DU-145 cells exposed to ethidium bromide is assessed by qPCR based on nuclear and mitochondrial gene primers (***see Notes 9-11***).

3.2.1. DNA isolation

1. Collect 1-5 X 10^6 DU-145 cells in a 15 mL tube and centrifuge the cell suspension at 520 G for 5 min.
2. Discard the supernatant, resuspend the pellet in 5 mL PBS, centrifuge the cell suspension at 520 G for 5 min.
3. Discard the supernatant and resuspend the pellet in 200 µL PBS.
4. Add 20 µL proteinase K (20 mg/mL) and 200 µL buffer AL as provided in the DNA Extraction Kit and vortex for 15 sec.
5. Incubate at 56 °C for 10 min.
6. Add 200 µL ethanol (96-100%) as recommended in the DNA Extraction Kit and vortex for 15 sec.

7. Transfer the content of the tube into a column as provided by the DNA Extraction Kit and centrifuge at 6000 G for 1 min.
8. Transfer the column to a clean 2 mL collection tube as provided by the DNA Extraction Kit and discard the tube with the filtrate.
9. Add 500 µL buffer AW1 as provided by the DNA Extraction Kit, centrifuge at 6000 G for 1 min and transfer the column to a clean tube.
10. Add 500 µL buffer AW2 as provided by the DNA Extraction Kit, centrifuge at maximum speed for 3 min and transfer the column to a clean tube.
11. Centrifuge at maximum speed for 3 min to remove any trace of ethanol.
12. Transfer the column to a 1.5 mL microcentrifuge tube, add 200 µL buffer AE as provided by the DNA Extraction Kit (***see Note 12***) and incubate for 1 min at room temperature (RT).
13. Recover DNA by centrifuging at 6000 G for 1 min and store the sample at -20 °C (***see Note 13***).

3.2.2. mtDNA quantification

1. Quantify DNA concentration and purity with a NanoVue™ Plus Spectrophotometer.
2. Dilute samples to a concentration of 5 ng/µL using PCR-grade distilled water.
3. Prepare a master mix composed of 4 µL LightCycler® FastStart DNA Master^{PLUS} SYBR Green I, 0.5 µL primer mix (5 µM for each primer) and 12.5 µL PCR-grade distilled water, per reaction (***see Note 14***).

4. Distribute the mix in a precooled qPCR capillary tube, add 3 µL DNA template (5 ng/µL) up to 20 µL total rection volume and centrifuge at 1000 G for 1 min to enable reagents mix with the template (***see Note 15***).
5. Insert the capillary tube in the LightCycler® 2.0 System and set thermal program (**Table 2**).
6. Results are obtained as cycle threshold (CT) for both genomic and mitochondrial amplicons. To evaluate mtDNA abundance, calculate the average of CT numbers obtained on genomic and mitochondrial amplicons, and plug them into the formula: $2^{(\text{average gDNA CT} - \text{average mtDNA CT})}$. A cell line is considered ρ^0 when CT obtained with mitochondrial primers is equivalent to CT in negative control conditions (**Figure 2**).

3.3. Isolation of ρ^0 cell clones by limiting dilution

If mtDNA can be detected after ethidium bromide treatment, we advise isolating ρ^0 cell clones by limiting dilution, as follows:

1. Briefly, add 100 µL complete DMEM supplemented with 50 µg/mL uridine and 100 µg/mL pyruvate per well in a 96-well plate except well A1 (***see Note 16***).
2. Seed 4 X 10^3 potential ρ^0 cells in 200 µL complete DMEM supplemented with 50 µg/mL uridine and 100 µg/mL pyruvate in well A1.
3. Add 100 µL complete DMEM supplemented with 50 µg/mL uridine and 100 µg/mL pyruvate to wells B1-H1 to obtain a final volume of 200 µL in all wells of column 1.

4. With an 8-channel micropipette, mix and transfer 100 µL from the first column (A1-H1) to the second column (A2-H2). Repeat such a 1:2 dilution across the plate (***see Note 17***) ultimately discarding 100 µL from the last column (A12-H12) (***see Note 18***).
5. With a 12-channel micropipette, add 100 µL complete DMEM supplemented with 50 µg/mL uridine and 100 µg/mL pyruvate to wells A1-A12 to obtain a final volume of 200 µL in all wells of row A.
6. With the same micropipette, mix and transfer 100 µL from the first row (A1-A12) to the second row (B1-B12). Repeat such a 1:2 dilution across the plate (***see Note 17***) ultimately discarding 100 µL from the last row (H1-H12) (***see Note 18***).
7. Typically, isolated clones will start growing after 1-2 weeks in standard culture conditions. At confluence, passage clones into two separate wells to test proliferation in complete DMEM supplemented with 100 µg/mL pyruvate but no uridine. Collect clones that present uridine auxotrophy and analyze mtDNA abundance by qPCR (***see Section 3.2***).

3.4. Expansion of donor cells, mitochondria isolation and purification

1. Expand 22Rv1 cells with complete RPMI 1640 medium in 75 cm^2 cell culture flasks until obtaining 25 X 10^6 cells or more.
2. Discard exhaust medium and harvest 22Rv1 cells in a 50 mL tube after incubating them with 3 mL Trypsin/EDTA for 5 min at 37 °C, then centrifuge at 520 G for 5 min at RT (***see Note 19***).
3. Discard the supernatant, wash cells 3X with ice-cold PBS and centrifuge at 520 G for 5 min at RT (***see Note 20***).

4. Resuspend the cell pellet in ice-cold hypotonic buffer (10 mM MOPS, 83 mM sucrose, pH 7.2), with a volume 7X estimated pellet volume (e.g., 700 µL hypotonic buffer for 100 µL pellet).
5. Transfer the cell suspension into a homogenizer-glass vessel and leave on ice for 2 min.
6. Disrupt cell membranes by performing between 8-10 strokes (***see Note 21***) in the homogenizer at 600 RPM (***see Note 22***).
7. Create an isotonic environment by adding the same volume (7X pellet volume) of ice-cold hypertonic buffer (30 mM MOPS, 250 mM sucrose, pH 7.2) to the cell suspension.
8. Mix and transfer the homogenate into a 15 mL tube.
9. Carry out 3 consecutive 5-min centrifugations at 4 °C and 1000 G. After each centrifugation, transfer the supernatant (which contains mitochondria) to a new tube and discard the pellet (which contains unruptured cells and other subcellular compartments) (***see Note 23***).
10. Centrifuge at 18,000 G and 4 °C for 2 min.
11. Discard the supernatant and resuspend the pellet in ice-cold buffer A.
12. Repeat this process until all mitochondria are sedimented in a single tube (***see Notes 24 and 25***). Keep mitochondrial extracts in ice.

3.5. Mitochondrial transfer (*see Note 22*)

1. Resuspend 2-3 X 10^6 ρ^0 cells in 2 mL complete DMEM supplemented with 50 µg/mL uridine and 100 µg/mL pyruvate.

2. Carefully lay the ρ^0 cell suspension on top of the mitochondria pellet and centrifuge at 520 G for 5 min to allow cells to mix with mitochondria.
3. Remove the supernatant and add 100 µL PEG solution (50 %), gently resuspend the pellet for 30 sec and allow to rest untouched for another 30 sec. This process facilitates the incorporation of mitochondria by cells.
4. Transfer the mixture into a 6-well plate with complete DMEM supplemented with 100 µg/mL pyruvate (but no uridine) and incubate at 37 $^{\circ}$C and 5 % CO_2. After 5-7 days, ρ^0 cells will succumb to the absence of uridine, enabling for the selection of transmitochondrial cybrids.

3.6. Analysis of mitochondrial purity

To verify the degree of heteroplasmy in transmitochondrial cybrids, restriction fragment length polymorphism (RFLP) based on a restriction enzyme that specifically recognizes a mtDNA palindrome from donor (but not recipient) cells is employed (***see Note 26***), as follows:

1. Expand 1-5 X 10^6 transmitochondrial cybrids in with complete DMEM supplemented with 100 µg/mL pyruvate and collect them upon detachment with 3 mL Trypsin/EDTA, and centrifugation at 520 G for 5 min.
2. Discard supernatant and resuspend the cell pellet in 5 mL PBS.
3. Extract DNA from the sample as described in **Section 3.2.1.**
4. Use 100 ng/mL DNA template in a standard PCR amplification protocol that, in the case of DU-145 and 22Rv1 cells, aims at generating a 1233-bp amplicon based on 5'-

GTGCCACCTATCACACCCCA-3’ and 5’-GAGTGGGGTTTTGCAGTCCTT-3’ forward and reverse primers (**Table 3**).

5. On ice, mix 1 µg amplified DNA, 5 µL 10X NEBuffer as provided by restriction enzyme kit, 1 µL *SacI*-HF® and nuclease-free water up to 50 µL total volume.
6. Gently mix by pipetting, and microfuge briefly at 500 G for 1 min.
7. Incubate at 37 ºC for 15 min (***see Note 27***) and at 65 ºC for 20 min to inactivate restriction enzymes.
8. Separate DNA fragments in a 1.5 % agarose gel (***see Note 2***).
9. Check the fragment pattern by exposing under UV light in the Azure 600® Imager (**Figure 3**).

4. Notes

1. Virtually equivalent disposables, reagents, equipment and software are available from a variety of alternative providers.
2. Ethidium bromide is a strong irritant as well as a powerful mutagenic agent, and hence should be handled with appropriate safety precautions.
3. This protocol is precisely tailored to DU-145 cells as recipient cells and 22Rv1 cells as mitochondrial donor cells, but minimal variations should be sufficient for it to be applicable to other cancer cell lines.
4. To avoid contaminations, the entire protocol should be performed under sterile conditions and with sterile (filtered or autoclaved) reagents.
5. Uridine and pyruvate are required to support the growth of mtDNA-depleted ρ^0 cells.
6. Cells are routinely grown at 37 ^{0}C under 5 % CO_2 in small (25 cm^2) or medium (75 cm^2) culture flasks.
7. Some cell lines might require alternative ethidium bromide dosing and/or administration schedules.
8. If mtDNA can still be detected, ρ^0 clones can be isolated from the cell population by limiting dilution (**see Section 3.3.**).
9. Some cell lines might develop resistance to ethidium bromide, which (at least in some cases) can be circumvented by increasing ethidium bromide concentration and shortening treatment duration.
10. Any qPCR primers that specifically recognize nuclear and mitochondrial genes can be used for this analysis. In this case, we designed qPCR primers with Primer Express 2.0 software tested them functionally in quantitative analysis.

11. DNA extracted from untreated cells provides a convenient positive control, pure water a convenient negative one.
12. Buffer AE can be replaced by distilled water.
13. DNA samples can be safely stored at -20 °C for 12-24 months in the absence of sizeable degradation.
14. Each sample should be analyzed for the abundance of both nuclear and mitochondrial amplicons.
15. Keep capillaries set in an ice-cold aluminum block.
16. Conditioned media from subconfluent DU-145 cell cultures can be employed to support the survival of single clones.
17. It is recommended to avoid the formation of bubbles during pipetting.
18. At this stage, all wells should contain 100 µL total volume.
19. Optimal collection strategy and centrifugation conditions may vary across different cell lines (e.g., trypsinization is not necessary for cells growing in suspension).
20. All steps for mitochondrial extraction and purification should be carried out with ice-cold reagents and ice-cold tubes.
21. Stroke refers to the action of pulling down the homogenizer glass tube to create a temporary vacuum while the pestle is rotating.
22. Cell membranes composition and strength vary across cell lines, implying that optimization may be required.
23. To avoid contamination with other cellular components or intact cells, supernatant should be collected as carefully as possible and only up to 75% of total volume, with the objective of leaving the pellet undisturbed.

24. This step ensures the precipitation of isolated mitochondria.
25. Mitochondrial purity can quickly be evaluated under light microscopy upon incubation of a small aliquot with 0.4% trypan blue in PBS (which marks nuclei, both inside and outside cells), 1:1 (v:v).
26. The restriction enzyme used for RFLP analysis strictly depends on donor cells. Here, we employed *SacI*-HF®, which specifically recognizes a palindrome in the mtDNA of 22Rv1 cells.
27. Restriction enzymes that display no unspecific (star) activity can be safely allowed to operate overnight.
28. Ethidium bromide is a strong irritant as well as a powerful mutagenic agent, and hence should be handled with the appropriate safety precautions.

5. Concluding remarks

Here, we provide a simple and fairly unexpensive method for generating transmitochondrial cybrids in cancer cells, based on (1) the establishment of mtDNA-depleted ρ^0 cells as recipient cells, (2) the extraction of intact mitochondria from donor cells, and (3) the delivery of mitochondria from donor cells to recipient cells. This approach has been successfully used to establish human DU-145 prostate cancer cells bearing mitochondria from human 22Rv1 prostate cancer cells {Soler-Agesta, 2023, 37010306} for the characterization of the mode of action of a novel immunotherapeutic agent known as PT-112{Soler-Agesta, 2022, 36010843;Yamazaki, 2020, 32117585;Karp, 2022, 35747193}, as well as mouse WT L929 fibroblasts bearing mitochondria from their a subline thereof with a detached phenotype (L929dt cells), for the study of mitochondrial metabolism {Catalán, 2015, 25949869;Marco-Brualla, 2019, 31330915; Marchi, 2020, 32559424}.

While the protocol presented herein is specifically tailored to DU-145 recipient and 22Rv1 donor cells, we expect it to be simply adaptable to other (cancer) cell lines with minor experimental variations. One of the limitations of this method emerges from the ability of some cell lines to acquire resistance to ethidium bromide. While in our settings simply increasing ethidium bromide concentration and shortening treatment duration was sufficient to circumvent such issue, an alternative solution consists in combining ethidium bromide with dideoxycytidine (ddC), a reverse transcriptase inhibitor that has been shown to inhibit mtDNA replication {Nelson, 1997, 9542530}. Moreover, suboptimal mtDNA depletion may be circumvented by isolating truly ρ^0 clones via limiting dilution. In this latter scenario, however, subsequent experimental assays should be performed on multiple independent control and ρ^0 clones to account for potential clone-dependent mtDNA-independent effects. Despite these and other

caveats, the protocol detailed herein stands out as a simple approach to study the influence of specific mtDNA genotypes on cancer cell functions, both *in vitro* and *in vivo*.

Acknowledgements. This work was partially supported the Spanish Association Against Cancer in Aragón (#PRDAR21487SOLE), proving financial support to RSA. CRY work is supported by the European Union-NextGenerationEU. The LG lab is/has been supported (as a PI unless otherwise indicated) by one NIH R01 grant (#CA271915), by two Breakthrough Level 2 grants from the US DoD BCRP (#BC180476P1, #BC210945), by a grant from the STARR Cancer Consortium (#I16-0064), by a Transformative Breast Cancer Consortium Grant from the US DoD BCRP (#W81XWH2120034, PI: Formenti), by a U54 grant from NIH/NCI (#CA274291, PI: Deasy, Formenti, Weichselbaum), by the 2019 Laura Ziskin Prize in Translational Research (#ZP-6177, PI: Formenti) from the Stand Up to Cancer (SU2C), by a Mantle Cell Lymphoma Research Initiative (MCL-RI, PI: Chen-Kiang) grant from the Leukemia and Lymphoma Society (LLS), by a Rapid Response Grant from the Functional Genomics Initiative (New York, US), by a pre-SPORE grant (PI: Demaria, Formenti), a Collaborative Research Initiative Grant and a Clinical Trials Innovation Grant from the Sandra and Edward Meyer Cancer Center (New York, US), by startup funds from the Dept. of Radiation Oncology at Weill Cornell Medicine (New York, US), by industrial collaborations with Lytix Biopharma (Oslo, Norway), Promontory (New York, US) and Onxeo (Paris, France), as well as by donations from Promontory (New York, US), the Luke Heller TECPR2 Foundation (Boston, US), Sotio a.s. (Prague, Czech Republic), Lytix Biopharma (Oslo, Norway), Onxeo (Paris, France), Ricerchiamo (Brescia, Italy), and Noxopharm (Chatswood, Australia).

Competing interests. LG is/has been holding research contracts with Lytix Biopharma, Promontory and Onxeo, has received consulting/advisory honoraria from Boehringer Ingelheim, AstraZeneca, OmniSEQ, Onxeo, The Longevity Labs, Inzen, Imvax, Sotio, Promontory, Noxopharm, EduCom, and the Luke Heller TECPR2 Foundation, and holds Promontory stock options. The other authors have no conflicts of interest to declare.

6. Legends to Figures

Figure 1. **Generation of transmitochondrial cybrids.** Recipient cells are treated with sublethal concentrations of ethidium bromide to eliminate mitochondrial DNA (mtDNA) and generate rho^0 cells. Once rho^0 recipient cells are established, intact mitochondria are isolated from donor cells and used to reconstitute a functional mitochondrial network in transmitochondrial cybrids.

Figure 2. **mtDNA quantification.** Wild-type (WT) human DU-145 prostate cancer cells were left untreated or exposed to 500 ng/mL ethidium bromide for 10 days as detailed in **Section 3.1.**, followed by the qPCR assessment of mitochondrial DNA (mtDNA) content, as detailed in **Section 3.2.** Results are represented as mean ± SEM from a single experiment performed in technical duplicates. ****$p<0.0001$ (unpaired Student's *t* test, as compared to untreated WT cells).

Figure 3. **Mitochondrial purity verification.** DNA was isolated from wild-type (WT) human DU-145 prostate cancer cells, WT human 22Rv1 prostate cancer cells and DU-145^{22Rv1} cybrids as detailed in **Section 3.2.1.**, followed by PCR for the amplification of a mitochondrial amplicon of 1233 bp, enzymatic digestion with *SacI*-HF® and product resolution on a 1.5% agarose gel, as detailed in **Section 3.6.**

7. Tables – Table 1

Gene	Primer	Position	Sequence
MT-CO2 (NC_012920)	*MT-CO2-FWD*	7858-7877	CGATCCCTCCCTTACCATCA
	MT-CO2-REV	7926-7904	CCGTAGTCGGTGTACTCGTAGGT
SDHA (AH008093)	*SDHA-FWD*	2641-2661	TCTCCAGTGGCCAACAGTGTT
	SDHA-REF	2712-2693	GCCCTCTTGTTCCCATCAAC

7. Tables – Table 1

Gene	Primer	Position	Sequence
MT-CO2	MT-CO2-FWD	7858-7877	CGATCCCTCCCTTACCATCA
(NC_012920)	MT-CO2-REV	7926-7904	CCGTAGTCGGTGTACTCGTAGGT
SDHA	SDHA-FWD	2641-2661	TCTCCAGTGGCCAACAGTGTT
(NC_000005.10)	SDHA-REV	2712-2693	GCCCTCTTGTTCCCATCAAC

Abbreviations: FWD, forward; MT-CO2, mitochondrially encoded cytochrome c oxidase subunit II; REV, reverse; SDHA, succinate dehydrogenase complex flavoprotein subunit A.

7. Tables – Table 2

Step	Temperature	Time	Cycles
Initial denaturation	95 ºC	10 min	1 cycle
Quantification	95 ºC	10 sec	55 cycles
	60 ºC*	10 sec	
	72 ºC	10 sec	
Melting Curve	95 ºC	1 sec	1 cycle
	65 ºC	15 sec	
	98 ºC	0 sec (rate: 0.1 ºC/s)	
Cooling	40 ºC	30 sec	1 cycle

*This temperature depends on the primers' sequence , and it can be calculated by using the following equation: Temperature = 2 (A+T) +4 (G+C).

7. Tables – Table 3

Step*	Time	Temperature
Initial denaturation	2 min	95 °C
Denaturation	30 sec	95 °C
Annealing	30 sec	Chosen according to the T_m of the primers used**
Extension	1-2 min***	72°C
Final extension	5 min	72°C

*Steps 2-4 were repeated for 29 cycles; **This temperature depends on the primers' sequence, and it can be calculated by using the following equation: Temperature = 2 (A+T) +4 (G+C); ***This time depending on the length of the amplicons: for fragments >1 Kbp 2 min are recommended.

8. References

Catalan, E., et al. (2015). MHC-I modulation due to changes in tumor cell metabolism regulates tumor sensitivity to CTL and NK cells. Oncoimmunology, 4, e985924. https://doi.org/10.4161/2162402x.2014.985924.

Cavaliere, A., et al. (2022). An in vitro approach to study mitochondrial dysfunction: A cybrid model. Journal of Visualized Experiments. https://doi.org/10.3791/63452.

Chavez, M., et al. (2023). Advances in CRISPR therapeutics. Nature Reviews. Nephrology, 19, 9–22. https://doi.org/10.1038/s41581-022-00636-2.

Craven, L., et al. (2017). Recent advances in mitochondrial disease. Annual Review of Genomics and Human Genetics, 18, 257–275. https://doi.org/10.1146/annurev-genom- 091416-035426.

DeBerardinis, R. J., & Chandel, N. S. (2020). We need to talk about the Warburg effect. Nature Metabolism, 2, 127–129. https://doi.org/10.1038/s42255-020-0172-2.

Diepstraten, S. T., et al. (2022). The manipulation of apoptosis for cancer therapy using BH3-mimetic drugs. Nature Reviews. Cancer, 22, 45– 64. https://doi.org/10.1038/s41568-021-00407-4.

Dora, D., et al. (2023). Non-small cell lung cancer patients treated with anti-PD1 immunotherapy show distinct microbial signatures and metabolic pathways according to progression-free survival and PD-L1 status. Oncoimmunology, 12, 2204746. https://doi. org/10.1080/2162402X.2023.2204746.

Gustafsson, C. M., et al. (2016). Maintenance and expression of mammalian mitochondrial DNA. Annual Review of Biochemistry, 85, 133–160. https://doi.org/10.1146/annurevbiochem-060815-014402.

Hanahan, D. (2022). Hallmarks of cancer: New dimensions. Cancer Discovery, 12, 31–46. https://doi.org/10.1158/2159-8290.Cd-21-1059.

Hanahan, D., & Weinberg, R. A. (2011). Hallmarks of cancer: The next generation. Cell, 144, 646–674. https://doi.org/10.1016/j.cell.2011.02.013.

Karp, D. D., et al. (2022). Phase I study of PT-112, a novel pyrophosphate-platinum immunogenic cell death inducer, in advanced solid tumours. EClinicalMedicine, 49, 101430. https://doi.org/10.1016/j.eclinm.2022.101430.

Kopinski, P. K., et al. (2021). Mitochondrial DNA variation and cancer. Nature Reviews. Cancer, 21, 431–445. https://doi.org/10.1038/s41568-021-00358-w.

Koppenol, W. H., et al. (2011). Otto Warburg's contributions to current concepts of cáncer metabolism. Nature Reviews. Cancer, 11, 325–337. https://doi.org/10.1038/nrc3038.

Kroemer, G., et al. (2023). Immunosurveillance in clinical cancer management. CA: a Cancer Journal for Clinicians. https://doi.org/10.3322/caac.21818.

Locasale, J.W., et al. (2011). Phosphoglycerate dehydrogenase diverts glycolytic flux and contributes to oncogenesis. Nature Genetics, 43, 869–874. https://doi.org/10.1038/ng.890.

Lunt, S. Y., & Vander Heiden, M. G. (2011). Aerobic glycolysis: Meeting the metabolic requirements of cell proliferation. Annual Review of Cell and Developmental Biology, 27, 441–464. https://doi.org/10.1146/annurev-cellbio-092910-154237.

Madigan, V., et al. (2023). Drug delivery systems for CRISPR-based genome editors. Nature Reviews. Drug Discovery, 22, 875–894. https://doi.org/10.1038/s41573-023-00762-x.

Marchi, S., et al. (2020). Ca(2+) fluxes and cancer. Molecular Cell, 78, 1055–1069. https://doi.org/10.1016/j.molcel.2020.04.017.

Marchi, S., et al. (2023). Mitochondrial control of inflammation. Nature Reviews. Immunology, 23, 159–173. https://doi.org/10.1038/s41577-022-00760-x.

Marco-Brualla, J., et al. (2019). Mutations in the ND2 subunit of mitochondrial complex I are sufficient to confer increased tumorigenic and metastatic potential to cancer cells. Cancers (Basel), 11. https://doi.org/10.3390/cancers11071027.

Medini, H., et al. (2020). Mitochondria are fundamental for the emergence of metazoans: On metabolism, genomic regulation, and the birth of complex organisms. Annual Review of Genetics, 54, 151–166. https://doi.org/10.1146/annurev-genet-021920-105545

Nelson, I., et al. (1997). Depletion of mitochondrial DNA by ddC in untransformed human cell lines. Somatic Cell and Molecular Genetics, 23, 287–290. https://doi.org/10.1007/ BF02674419.

Neupert,W. (2016).Mitochondrial gene expression: A playground of evolutionary tinkering. Annual Review of Biochemistry, 85, 65– 76. https://doi.org/10.1146/annurev-biochem-011116-110824.

Newman, L. E., & Shadel, G. S. (2023). Mitochondrial DNA release in innate immune signaling. Annual Review of Biochemistry, 92, 299–332. https://doi.org/10.1146/annurev-biochem-032620-104401.

Oldan, J. D., et al. (2023). Increased tryptophan, but not increased glucose metabolism, predict resistance of pembrolizumab in stage III/IV melanoma. Oncoimmunology, 12, 2204753. https://doi.org/10.1080/2162402X.2023.2204753.

Petroni, G., et al. (2021). Immunomodulation by targeted anticancer agents. Cancer Cell, 39, 310–345. https://doi.org/10.1016/j.ccell.2020.11.009.

Porporato, P. E., et al. (2018). Mitochondrial metabolism and cancer. Cell Research, 28, 265–280. https://doi.org/10.1038/cr.2017.155.

Rackham, O., & Filipovska, A. (2022). Organization and expression of the mammalian mitochondrial genome. Nature Reviews. Genetics, 23, 606–623. https://doi.org/10.1038/s41576-022-00480-x.

Roy, A., et al. (2022). Mitochondrial DNA replication and repair defects: Clinical phenotypes and therapeutic interventions. Biochimica et Biophysica Acta - Bioenergetics, 1863, 148554. https://doi.org/10.1016/j.bbabio.2022.148554.

Schwenck, J., et al. (2023). Advances in PET imaging of cancer. Nature Reviews. Cancer, 23, 474–490. https://doi.org/10.1038/s41568-023-00576-4.
Soler-Agesta, R., et al. (2022). PT-112 induces mitochondrial stress and immunogenic cell death, targeting tumor cells with mitochondrial deficiencies. Cancers (Basel), 14. https://doi.org/10.3390/cancers14163851.
Soler-Agesta, R., et al. (2023). Transmitochondrial cybrid generation using cancer cell lines. Journal of Visualized Experiments. https://doi.org/10.3791/65186.
Sprooten, J., et al. (2023). Trialwatch:Chemotherapy-induced immunogenic cell death in oncology. Oncoimmunology, 12, 2219591. https://doi.org/10.1080/2162402X.2023.2219591.
Stewart, J. B., & Chinnery, P. F. (2021). Extreme heterogeneity of human mitochondrial DNA from organelles to populations. Nature Reviews. Genetics, 22, 106–118. https://doi.org/10.1038/s41576-020-00284-x.
Stine, Z. E., et al. (2022). Targeting cancer metabolismin the era of precision oncology. Nature Reviews. Drug Discovery, 21, 141–162. https://doi.org/10.1038/s41573-021-00339-6.
Thompson, C. B., et al. (2023). A century of the Warburg effect. Nature Metabolism, 5, 1840–1843. https://doi.org/10.1038/s42255-023-00927-3.
Vander Heiden, M. G., et al. (2009). Understanding the Warburg effect: The metabolic requirements of cell proliferation. Science, 324, 1029–1033. https://doi.org/10.1126/science.1160809.
Vaupel, P., & Multhoff, G. (2021). Revisiting the Warburg effect: Historical dogma versus current understanding. The Journal of Physiology, 599, 1745–1757. https://doi.org/10.1113/jp278810.
Villiger, L., et al. (2024). CRISPR technologies for genome, epigenome and transcriptome editing. Nature Reviews. Molecular Cell Biology. https://doi.org/10.1038/s41580-023-00697-6.
Vitale, I., et al. (2023). Apoptotic cell death in disease-current understanding of the NCCD2023. Cell Death and Differentiation, 30, 1097–1154. https://doi.org/10.1038/s41418-023-01153-w.
Vringer, E., & Tait, S. W. G. (2023). Mitochondria and cell death-associated inflammation. Cell Death and Differentiation, 30, 304–312. https://doi.org/10.1038/s41418-022-01094-w.
Vyas, S., et al. (2016). Mitochondria and Cancer. Cell, 166, 555–566. https://doi.org/10.1016/j.cell.2016.07.002.
Warburg, O. (1956a). On respiratory impairment in cancer cells. Science, 124, 269–270.
Warburg, O. (1956b). On the origin of cancer cells. Science, 123, 309–314. https://doi.org/10.1126/science.123.3191.309.
Warburg, O., & Minami, S. (1923). Versuche an € Uberlebendem Carcinom-gewebe. Klinische Wochenschrift, 2, 776–777. https://doi.org/10.1007/BF01712130.
Warburg, O., et al. (1924). € Uber den stoffwechsel der carcinomzelle. Naturwissenschaften, 12,1131–1137.
Yamazaki, T., et al. (2020a). Mitochondrial DNA drives abscopal responses to radiation that are inhibited by autophagy. Nature Immunology, 21, 1160–1171. https://doi.org/10.1038/s41590-020-0751-0.
Yamazaki, T., et al. (2020b). PT-112 induces immunogenic cell death and synergizes with immune checkpoint blockers in mouse tumor models. Oncoimmunology, 9, 1721810. https://doi.org/10.1080/2162402x.2020.1721810.
Yang, X., et al. (2019). Mitochondrial DNA mutation, diseases, and nutrient-regulated Mitophagy. Annual Review of Nutrition, 39, 201–226. https://doi.org/10.1146/annurev-nutr-082018-124643.
Yankeelov, T. E., et al. (2014). Quantitative multimodality imaging in cancer research and therapy.Nature Reviews. Clinical Oncology, 11, 670–680. https://doi.org/10.1038/nrclinonc.2014.134.
Yuan, J., & Ofengeim, D. (2023). A guide to cell death pathways. Nature Reviews. Molecular Cell Biology. https://doi.org/10.1038/s41580-023-00689-6.
Zhang, H., et al. (2021). Perfecting targeting in CRISPR. Annual Review of Genetics, 55, 453–477. https://doi.org/10.1146/annurev-genet-071719-030438.
Zong, W. X., et al. (2016). Mitochondria and Cancer. Molecular Cell, 61, 667–676. https://doi.org/10.1016/j.molcel.2016.02.011.

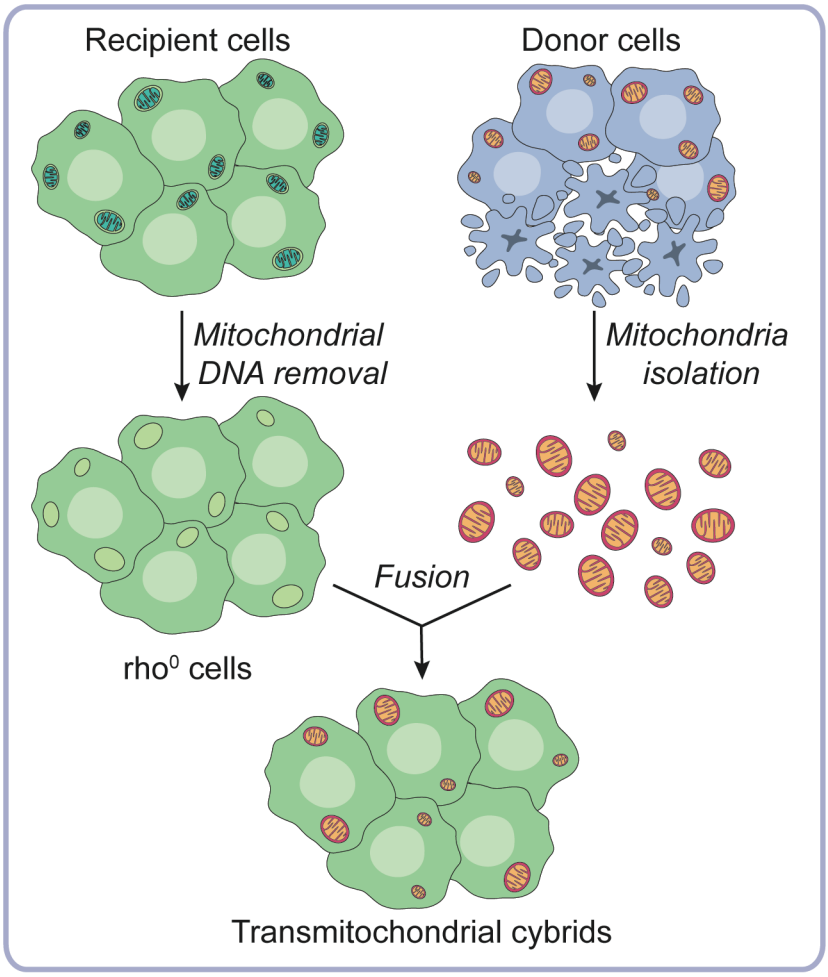
Recipient cells
Donor cells
Mitochondrial DNA removal
Mitochondria isolation
Fusion
rho0 cells
Transmitochondrial cybrids

Figure 1

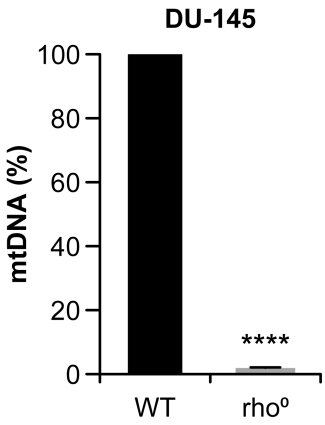

Figure 2

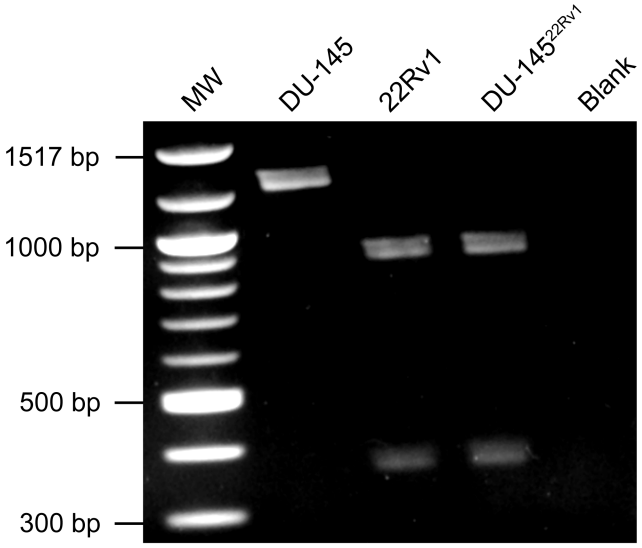

Figure 3